Available online at www.derpharmachemica.com

ISSN 0975-413X
CODEN (USA): PCHHAX

Der Pharma Chemica, 2016, 8(4):122-132
(http://derpharmachemica.com/archive.html)

Inhibition effect of aminotriazole derivative on the corrosion of Cu-40Zn alloy in 3%NaCl solution in presence of Sulphide ions

Benmessaoud M.[a,b,c], Serghini Idrissi M.[a], Labjar N.[a,d], Rhattas K.[c], Damej M.[c], Hajjaji N.[c], Srhiri A.[c] and El Hajjaji S.[a*]

[a]*LS3ME, Faculté des Sciences, Mohammed V University in Rabat, Av. Ibn Battouta, B.P. 1014, M-10000 Rabat, Morocco*
[b]*Laboratoire d'Energétique, Matériaux et Environnement, Ecole Supérieure de Technologie, Mohammed V University in Rabat, B.P. 227 Salé médina Maroc*
[c]*Laboratoire d'Electrochimie, des Etudes de Corrosion et d'Environnement, Faculté des Sciences, BP 133 Kenitra Maroc*
[d]*Laboratoire de mécanique, Procédés et Process Industriels, Mohammed V University in Rabat, ENSET, Rabat, Morocco*

ABSTRACT

The effect of synthesis N-decyl-3-amino-1,2,4-triazole noted (TN_{10}) on the corrosion behavior of copper-zinc 60 - 40 (Brass) in NaCl 3% solution has been investigated at 298 K in presence and in absence of sulphide ions using weight loss measurements, potentiodynamic polarization, impedance spectroscopy (EIS) methods and surface characterization. Polarization measurements showed that the organic compound investigated act as mixed type inhibitor retarding both anodic and cathodic reaction. The impedance results show a change on the corrosion mechanism of brass in the presence of inhibitor. Appropriate electric equivalent circuit model was used to calculate the impedance parameters. Changes in the impedance parameters are related to the adsorption of organic inhibitor on the metal surface, leading to the formation of protective film. This film depends on the immersion time. Inhibition efficiencies obtained from different studied methods are in good agreement. Inhibition efficiency up to 95% can be obtained at 0.5 mM of inhibitor and after 60 min of immersion time.

Keywords*:* Brass, Triazole, Inhibitor, Efficiency, Polarization curve, Electrochemical Impedance

---

INTRODUCTION

According to their good corrosion resistance in neutral aggressive media and their ability of processing, brasses are widely used in industries, particularly as condensers and heat exchangers in power plants [1-3]. When brass is dipped in a media containing chloride ion, an insoluble film of cuprous chloride is adsorbed on the brass surface. The copper ions can pass into the solution by disproportionate reaction or it can dissolve with the formation of complexes with $CuCl_2$ [4, 5]. The formation of stable Cu_2O is possible inside the pores of CuCl layer. As a result, the brass surface becomes enriched with copper while being impoverished by zinc during corrosion [5]. These changes make brass surface less resistant to corrosion than copper in media containing chloride [6]. Indeed, in the presence of oxygen, chlorides, sulphates or nitrates ions are exposed to localized corrosion [7, 8]. However, the corrosion resistance of these alloys depends not only on their chemical composition but also on the environment medium nature [9-14].

Substantial improvement in brass passivity can be achieved using corrosion inhibitors. Most of the well-known corrosion inhibitors are organic compounds containing polar groups having nitrogen, sulfur and/or oxygen atoms and heterocyclic compounds with polar functional groups and conjugated double bonds [15-18].

The aim of this work is to study the effect of addition of N-decyl-3-amino-1,2,4-triazole (TN10) on the corrosion resistance of the Cu-40Zn in 3% NaCl solution in the presence and in the absence of sulphide ions. Electrochemical techniques such as polarization curves, electrochemical impedance spectroscopy (EIS) combined with weight loss measurements and surface characterization have been used to characterize the inhibiting effect.

MATERIALS AND METHODS

2.1. Materials

The working electrode was commercial brass Cu60Zn40. The chemical composition (wt %) was: 60Cu%, 38Zn%, 2Pb.

2.2. Solutions

The solutions used in this study were prepared using reagent grade chemicals and ion-exchanged water. The standard aggressive medium was 3% NaCl. The sulphide ions S^{2-} were added as Na_2S in solution to the concentration of 2 ppm.

2.3. Inhibitor

The TN_{10} (Figure 1) was prepared under the conditions of the transfer catalysis solid-liquid phase alkylation of 3-amino-1,2,4-triazole using as alkylating agent of alkyl halide in dimethyl formamide at ambient temperature and as base potassium carbonate, bromide, tetra-n-Buthyl ammonium as catalyst.

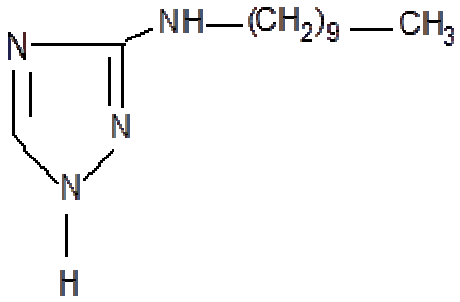

Figure 1: Chemical structure of the investigated N-decyl-3-amino-1,2,4-triazole (TN_{10})

2.4. Weight loss measurement

Gravimetric experiments were performed with rectangular Brass coupons (5 cm × 3 cm× 0.3 cm). The solution volume was 300 mL of 3%NaCl solution, with and without inhibitor during 5 days at room temperature (298 K). At the end of the tests, the specimens were carefully washed with distilled water and adherent corrosion products were removed by immersing the coupons in 6% H_2SO_4 for 20s. Then, the coupons were rinsed with distilled water, cleaned with acetone, dried and then weighted. Duplicate experiments were performed in each case and the mean value of the weight loss was reported.

The corrosion rate *CR* and the percentage of inhibition efficiency E_{CR} (*%*) over the exposure period were calculated using the following equations [19]:

$$CR = 87.6 \text{ x } \frac{\text{W}}{\text{D x A x t}} \quad (1)$$

Where W is the weight-loss in (mg), t the immersion time in (hours), A the coupons area in (cm^2), D the density of the specimen in (g/cm^3).

$$E_{CR} = \frac{CR - CR_{inh}}{CR} x100 \quad (2)$$

Where *CR* and CR_{inh} are the corrosion rate values in the absence and in the presence of inhibitor respectively.

2.5. Potentiodynamic polarization method

The measurements were carried out in a three electrodes electrochemical cell with a platinum counter electrode and an Ag/AgCl electrode as reference. The working electrode was a rotating disk consisting of cylindrical (60Cu-Zn) samples with 0.78cm^2 cross-sectional area. The rate of rotating electrode was 1000rpm.The potential scan rate was 1

mV/s. For all the experiments, the surface pre-treatment was carried out by grinding with emery paper SiC (grades 120, 600 and 1200) and rinsed with distilled water before use.

The potential polarization studies were carried out using on PGZ100 potentiostat. The working electrode was initially immersed in aerated solution at room temperature and allowed to stabilize for 1 hour at open circuit potential. Then the cathodic and anodic curves were recorded.

The inhibition efficiency were calculated using the following formula:

$$E\% = \frac{i_{corr}^{0} - i_{corr}}{i_{corr}^{0}} x100 \qquad (3)$$

Where i_{corr}^{0} and i_{corr} are the corrosion current densities obtained in the absence and in the presence of the inhibitor, respectively.

2.6. Electrochemical impedance spectroscopy (EIS)

Electrochemical impedance spectra (EIS) were carried out at the open-circuit potential E_{corr} using a potentiostat PGZ100. The measuring ranged from 100 kHz down to 10 mHz, were applied in these tests which were performed in the potentiostatic mode at the corrosion potential after 1 hour of immersion time. Data were presented as Nyquist plots. E % were calculated using the following equation:

$$E\% = \frac{R_{ct}^{i} - R_{ct}^{0}}{R_{ct}^{0}} x100 \qquad (4)$$

where R^{i}_{ct} and R^{0}_{ct} are the charge transfer resistance in the presence and the absence of TN_{10}, respectively.

2.5. Surface analysis

The surface morphology of the electrode was performed by using scanning electron microscope (SEM: Leica stereoxam 440). After 24 hours of immersion with and without inhibitor, the specimens were cleaned with double distilled water and dried at room temperature before to be examined by SEM technique.

RESULTS AND DISCUSSION

3.1. Weight-Loss Method

Table 1 Shows the corrosion rate and inhibition efficiency of Brass by weight-loss measurements at different concentrations of inhibitor in NaCl 3% solution in the presence and in the absence of sulphide ions at room temperature (298K). The inhibition efficiency increases and *CR* decreases with the increase of inhibitor concentration. The optimal efficiency reaches 94.5% and 95.1% at 0.5 mM concentration of TN_{10} without and with sulphide ions respectively.

Table 1: Weight-Loss results for Brass in NaCl 3% solution in the presence and in the absence of sulphide ions at different concentrations of TN_{10} at 298K

Solution	[TN_{10}] (mM)	*CR* (×10^{-2} mm·$year^{-1}$)	E_{CR} (%)
3%NaCl	0	5.06	-
	0.5	0.28	94.5
3%NaCl+2ppm S^{2-}	0	10.73	-
	0.01	2.75	57.7
	0.05	2.15	72.5
	0.07	1.08	85.3
	0.1	0.55	89.4
	0.5	0.47	95.1

3.2. Potentiodynamic polarization method

3.2.1. Effect of sulphide ions

3.2.1.1. Polarization curves

Figure 2 presents the cathodic and anodic polarization curves obtained separately from a potential close to E_{corr} in the absence or in the presence of 2 ppm of S^{2-}.

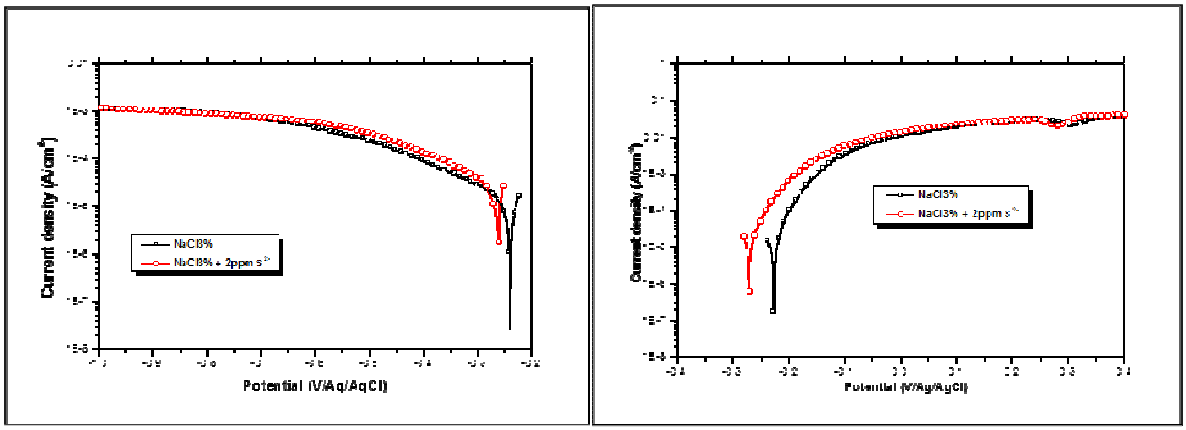

Figure 2: Cathodic and anodic polarization curves of brass in aerated 3%NaCl medium without and with 2ppm of S^{2-} at 298K; Ω = 1000rpm; │dE/dt│=1mv/s

For cathodic polarization curves, the addition of sulphide ions was accompanied by an increase of the current density values near to the corrosion potential. In the presence of sulphide ions, the cathodic curve showed a shape similar to that obtained in the 3% NaCl solution, and present a current diffusion plateau characteristic of the dissolved oxygen transport to the electrode.

The corrosion current density was determined by Tafel extrapolation of the current density-potential curve after correction of diffusion, by using the following relation (5) [20, 21]:

$$\frac{1}{I} = \frac{1}{I^*} + \frac{1}{I_1} \qquad (5)$$

Where:
I: current density at mixed process.
I^* : corrected current density.
I_1: limited current density.

Values of electrochemical parameters such as corrosion potential (E_{corr}), cathodic Tafel slop (b_c) and corrosion current density (I_{corr}) are given in **Table 2**.

Table2. Corrosion inhibition parameters of brass in aerated 3% NaCl solution without and with addition of 2 ppm of S^{2-} at 25°C.

Solution	E_{corr} (mV/Ag-AgCl)	I_{corr}(µA/cm^2)	b_c(mV/dec)
NaCl 3%	-232	12.93	-176
NaCl 3% + 2ppm S^{2-}	-262	27.41	-214

The corrosion current density increases from 12.93 µA cm^{-2} without sulphide to 27.41 µA cm^{-2} with 2ppm of sulphide, corresponding to 55% increase of the corrosion rate. This result indicates that sulphide addition induces an acceleration of the dissolution mechanism of brass.

For the anodic branch, we note an increase of the current density values. This shows the accelerating effect of the sulphide ions on the anodic reaction. This current exhibits a maximum and then increased again. This maximum current, was explained by the formation of CuCl, Cu_2O, and/or Cu_2S film that protects the copper from a further dissolution as the diffusion limiting current by $CuCl_2$ [22-24] .The subsequent current increase is due to the dissolution of copper in cupric ions [25–29].

3.2.1.2. Electrochemical impedance spectroscopy
Figure 3(A) presents Nyquist plot of impedance spectra of Cu–40Zn alloy in aerated 3% NaCl solution with and without 2 ppm of sulphide at corrosion potential (E_{corr}) after 1 h of stabilisation time.

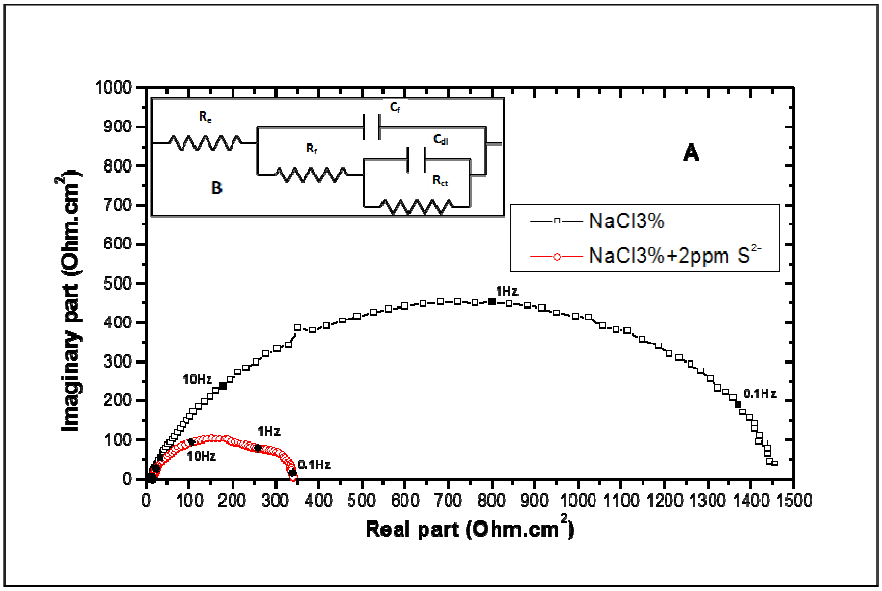

Figure 3: Impedance diagrams of Cu–40Zn in the corrosion test solution in the absence and the presence of sulphide ions after 60 min of stabilisation period. Ω = 1000 rpm

The impedance spectra in the absence of sulphide ions presents one capacitive loop that can be attributed to a charge transfer process [30, 31]. The value of associated resistance is about 1.41 kΩ.cm^2. The capacity is in the order of 112µF.cm^{-2}.

On adding sulphide ions to the 3%NaCl solution, the impedance diagram changes in shape and size. The diagram may be split into two capacitance loops. However, in contrast to the case of copper electrode as working electrode [32**]**, the addition of sodium sulphate induces a new time constant. In other study [33], the impedance spectra in presence of pollutant such as ammoniac present two capacitive loops and the first loop can be attributed to a charge transfer process. The electrical equivalent circuit consists of two parallel R and C as proposed in Figure 3B. Re represents the electrolyte resistance, C_{film} and R_{film} represent the coating capacitance and the resistance related to the electrolyte passing through the coating defect and the characteristic frequency at the maximum of the imaginary part, respectively. C_{dl} is the double layer capacitance, and R_t is the charge transfer resistance. The impedance parameters were calculated and listed in Table 3.

The circuit elements are defined as follows:
R_e : Electrolyte resistance (Ω cm^2)
R_f : Film resistance due to the ionic conduction through inhibitor layer (Ω cm^2)
C_f : Film capacitance due to the electronic insulating property (F cm^{-2})
R_{ct} : charge transfer resistance (Ω cm^2)
C_{dl} : Double layer capacitance at the metal electrolyte interface (F cm^{-2})

Table 3: Parameters determined from diagrams presented in Fig. 3

Solution	R_e (Ω cm^2)	R_f (kΩ cm^2)	C_f (µF cm^{-2})	R_t (kΩ cm^2)	C_{dl} (µF cm^{-2})
NaCl 3%	13.48	-	-	1.41	112
NaCl 3% + 2ppm S^{2-}	12.52	277.4	194	0.047	3 609.4

According to the results presented in table 2, the value of the polarization resistance increases from 140 Ω cm^2 without sulphides to 320 Ω cm^2 with sulphide ions. These results are in good agreement with other work [34-36] showing that the presence of a small quantity of sulphide has a large catalytic effect on the oxygen reduction reaction. The presence of Cu_2S, which is an electronic conducting species, in the corrosion products layer, induce a rise to a double layer capacity [32].

3.2.2. Effect of N-decyl-3-amino-1,2,4-triazole (TN_{10})
3.2.2.1. Polarization curves
The cathodic and anodic polarization curves of brass obtained in 3% NaCl solution containing or not sulphide ions and with various TN_{10} concentrations are presented in Figures 4A and 4B. The range of TN_{10} concentrations investigated in this work was limited since the solubility of the synthesized compound was quite low (between 0.5

and 0.7 mM). All of these curves were obtained after 1 h of immersion time of the electrode in the electrolytic solution at open circuit potential (*E*oc).

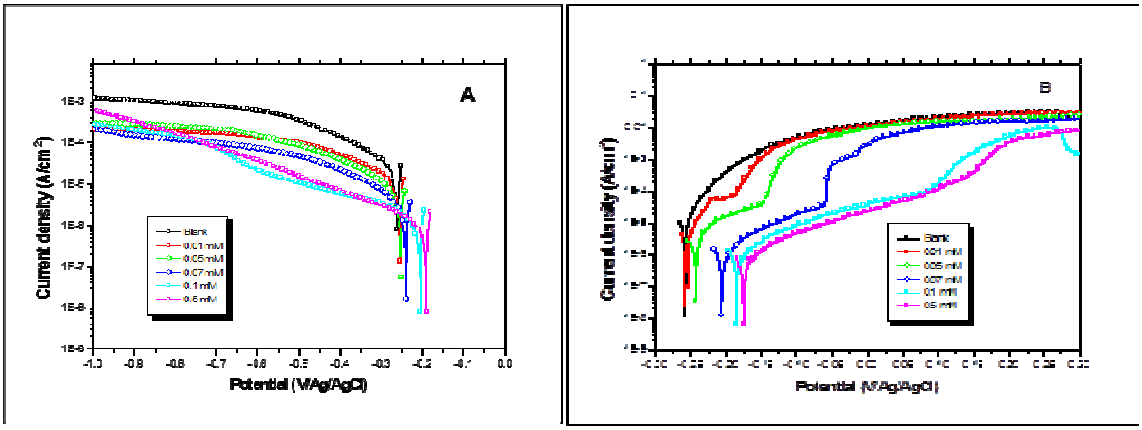

Figure 4: Cathodic and Anodic polarization curves of brass in aerated 3%NaCl without and with sulphide ions in the presence of TN_{10} at 298K; Ω=1000rpm; │dE/dt│= 1mv/s

Addition of the investigated compound to the solution induces a decrease of cathodic and anodic current densities for all the concentration with displacement of the corrosion potential towards more positive values. For 0.5 mM of TN_{10}, a large linear domain is obtained, indicating a modification of the cathodic process kinetic control. Values of electrochemical parameters such as corrosion potential (E_{corr}), cathodic tafel slope (b_c), corrosion current density value (I_{corr}) and inhibition efficiencies (E %) for various concentrations of TN_{10} are given in Table 4.

Table 4: Corrosion inhibition parameters of brass in aerated 3% NaCl solution without and with addition of TN_{10} at various concentrations at 298K

Solution	[TN_{10}] (mM)	E_{corr} (mV/Ag-AgCl)	I_{corr} (µA/cm²)	b_c (mV/dec)	E (%)
3%NaCl+2ppm S^{2-}	Blank	-262	27.4	-214	-
	0.01	-255	11.2	-251	59.3
	0.05	-253	6.9	-219	74.9
	0.07	-240	3.4	-220	87.6
	0.1	-206	1.85	-204	93.3
	0.5	-191	0.85	-146	96.9

These results show that the values of cathodic Tafel slope (*bc*) change with inhibitor concentrations. The inhibition efficiency of TN_{10} attained a maximum value of 96.9% at 0.5 mM. The inhibition efficiency increases with increasing concentration of inhibitor, indicating that a higher surface coverage was obtained in a solution with the optimum concentration of inhibitor.

Anodic polarisation curves presented in Figure 5B show also a change in the shape of polarisation curves may correspond to a likely change in the nature and rate of anodic reaction. Indeed, the addition of TN_{10} at different concentrations in a corrosive solution in presence of sulphide ions, leads to a substantial decrease of the anodic current density values and corrosion potential shift towards positive one. This confirms the establishment of a passive state of the brass in the presence of TN_{10}, which reduces its dissolution in 3%NaCl solution in the presence and in the absence of sulphide ions.

For a TN_{10} concentration higher than 0.07 mM, the anodic curve is modified and presents a passive domain, which is clearly observed compared to blank essay. This effect can be explained by the fact that the product tested acts by adsorption on the surface of the material and contributes to an establishment of anodic film formation. This passivity is broken with anodic overtension. This effect can be attributed to the destruction or the desorption of the film formed by the TN_{10} on the surface of the electrode.

Figure 5 shows the variation of θ as a function of log *C* of TN_{10}, where θ is the surface coverage.

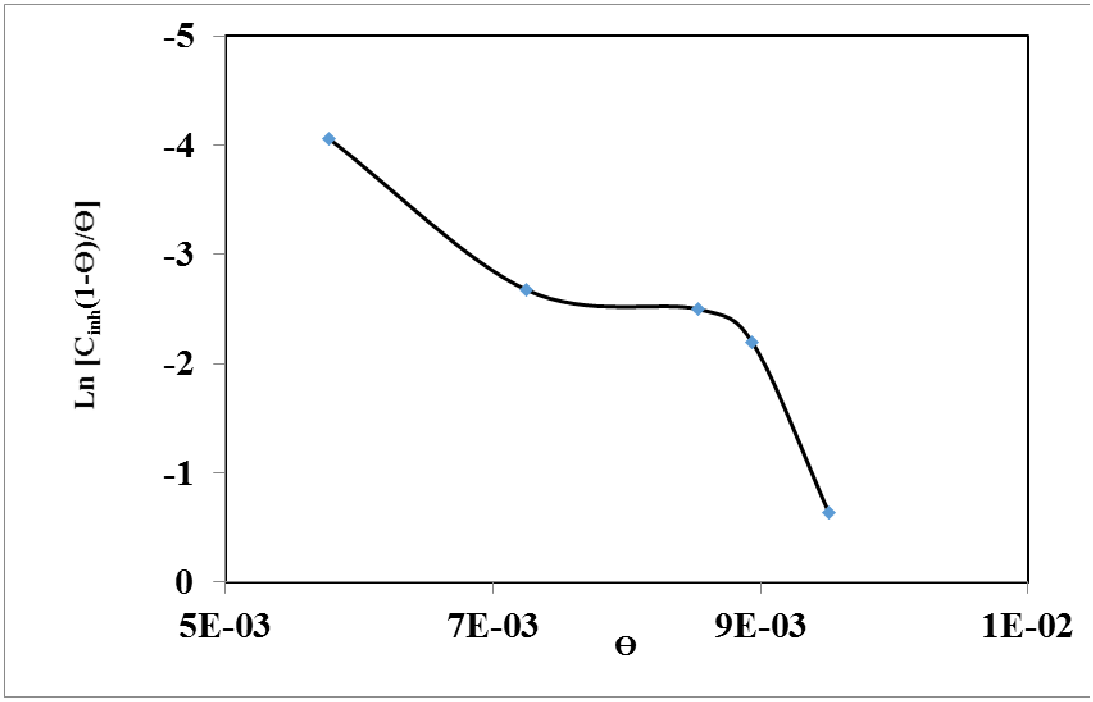

Figure 5. Frumkin isotherm model of TN_{10} on Brass surface

The TN10 adsorbs on the Brass surface according to the Frumkin isotherm model and the free energy of adsorption, is equal to -30 kJ/mol.

3.2.2.2. Electrochemical impedance spectroscopy

Figure 6 shows the impedance spectra collected on Brass electrode in 3% NaCl solution with sulphide ions in the presence of different TN_{10} concentrations. The insert presents high frequency domain of EIS in enlarged scale. By adding of inhibitor, the impedance display of the electrode in TN_{10} containing the solution changes in shape and size, on the other hand it can be noticed that the impedance modulus increased in the presence of inhibitor. This impedance reaches approximately 80 kΩ cm^2 in the presence of 0.5 mM TN_{10}. These diagrams show the presence of at least two different contributions. The first is located in the high frequency (R_f-C_f) and can be associated with the character of the dielectric film formed by the corrosion products, reinforced by the presence of inhibitor and the ionic conduction through the film pores. The second, at medium frequencies (R_{ct}-C_{dl}) attributed to the ability of the double layer at the electrolyte-Brass interface at the bottom of the pores, coupled charge transfer resistance. However, these diagrams can not be explained with only two R and C circuits displayed in Figure 4, and thus, a third R–C circuit was added. The use of such an electrical equivalent circuit is in agreement with the previous works [32]. Finally, at low frequencies, a third input of which the elements (C_F-R_F) are related to the oxidation–reduction contribution of the corrosion products. Moreover, the values determined for (C_F-R_F) from the numerical simulations of the ac diagrams are not discussed in the text since it appears that they are scattered probably due to the fact that they are likely ascribed to corrosion products.

The results of non-linear regression calculation with a Z view method are superimposed in Figure 6, and the calculated variables are presented in Table 5.

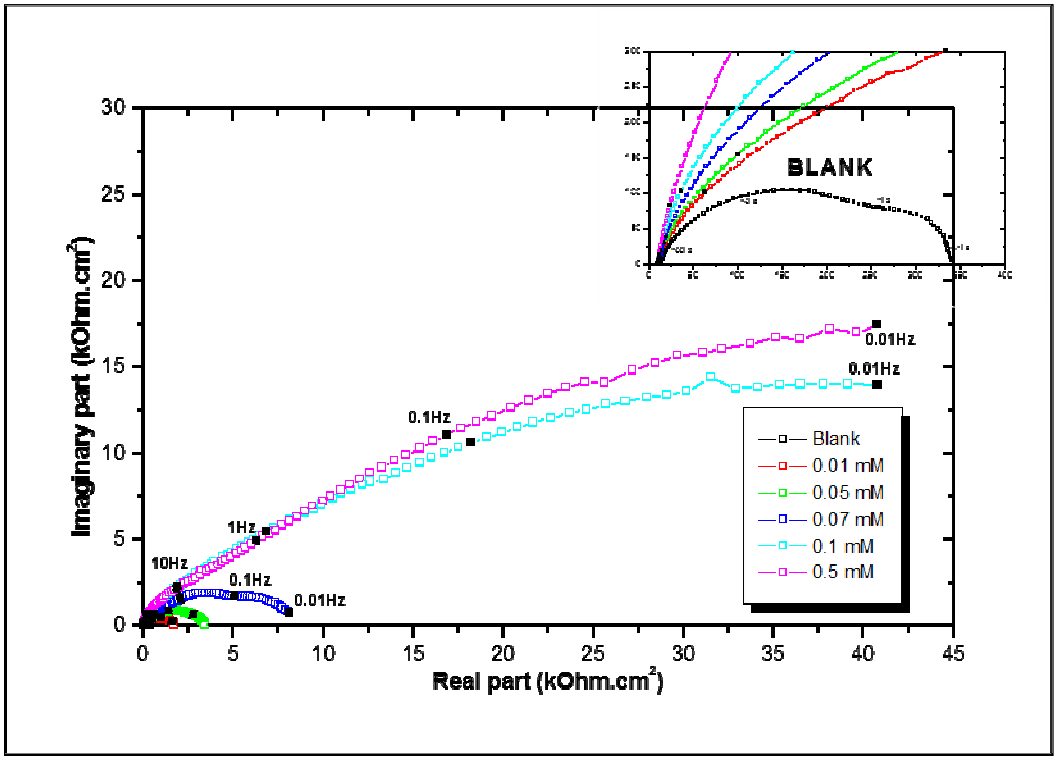

Figure 6: Impedance diagrams of Cu–40Zn in aerated 3%NaCl, with sulphide ions, in the presence of various concentrations of TN_{10} at 298K; Ω = 1000rpm

Table 5: Parameters determined by non-linear regression of the results presented in Figure 6

Solution	[TN_{10}] (mM)	R_e(Ω cm²)	R_f (kΩ cm²)	C_f (µF cm⁻²)	R_{ct}(kΩ cm²)	C_{dl}(µF cm⁻²)	*E(%)*
3%NaCl+2ppm S^{2-}	0	12.52	284.5	99.4	146.2	1193	-
	0.01	10.11	697.1	9.13	1.995	75.52	92.6
	0.05	10.34	904.2	6.226	3.980	71.44	96.3
	0.07	11.41	1.253	4.522	6.659	63.17	97.2
	0.1	10.08	1.330	1.071	55 910	56.92	99.7
	0.5	13.15	2.652	0.538	100 200	35.69	99.8

The film resistance R_f increases, globally, with TN_{10} concentration whereas the C_f value decreases. The surface film formed in presence of TN_{10} is therefore thicker and less permeable. From the R_t values calculated by a non-linear regression, the inhibiting efficiency increases with TN_{10} concentration. The inhibiting efficiency is evaluated according to the equation (4). The inhibiting efficiency was close to 99.8% when 0.5Mm TN_{10} was added in the sulphide containing test solution. Its efficiency is already as high as 90% when only 0.01mM TN_{10} was present in the solution. The inhibiting efficiency determined by the EIS is close to that evaluated from the cathodic polarization curves. The value of C_d decreases with TN_{10} concentration, which will be explained by a smaller area of brass directly in contact with electrolyte beneath the corrosion product layer or a less conducting nature of this film.

Figure 7 presents the effect of the immersion time on the impedance spectra at the corrosion potential. The inhibitor concentration was set at 0.5 mM. The shape of these curves is very similar to that obtained when varying the inhibitor concentration. The polarization resistance (determined at the low frequency limit of the impedance spectrum) changes from about 0.1M Ωcm² after 1 h to approximately 0.22 Ωcm² after 24 h immersion. This increase illustrates the protective effect of the TN_{10}, which is reinforced with the immersion time.

The results of non-linear regression calculation with a Zview method are superimposed in Figure 7, and the calculated variables are presented in Table 6.

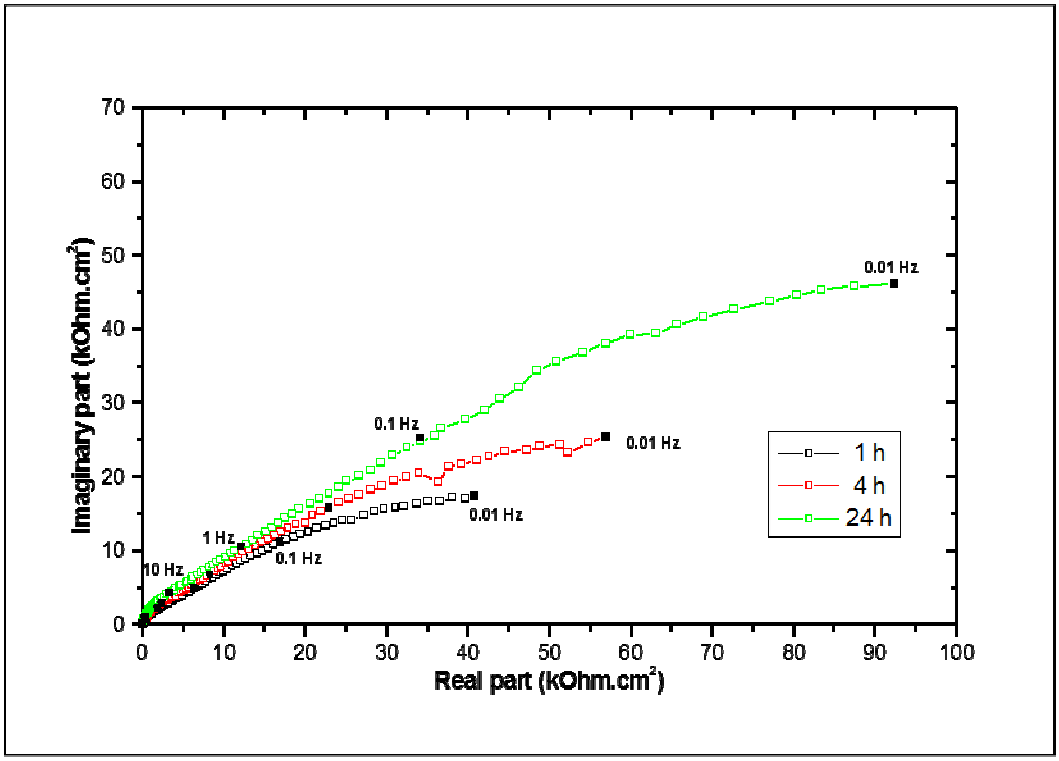

Figure 7: Impedance diagrams of Cu–40Zn in aerated 3%NaCl with sulphide ions in the presence of 0.5 mM of TN_{10} at various immersion times at 298K; Ω = 1000rpm

Table 6: Parameters determined by non-linear regression of the results presented in Figure 7

Time (h)	R_e (Ω cm²)	R_f (kΩ cm²)	C_f (µF cm⁻²)	R_{ct} (kΩ cm²)	C_{dl} (µF cm⁻²)
1	13.15	2.652	0.538	100 200	35.69
4	10.32	4.375	0.509	150 300	26.46
24	10.21	7.835	0.507	217 600	18.28

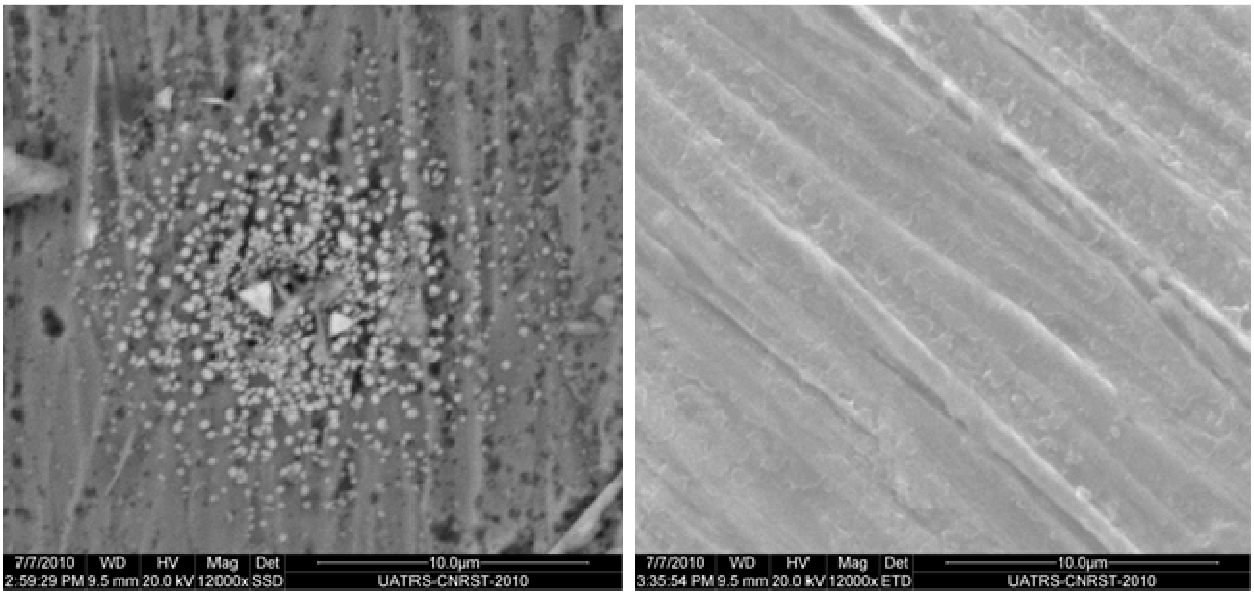

Figure 8: SEM picture of Cu–40Zn electrode surface after 24 h immersion in aerated 3%NaCl in the presence of sulphide ions, (A) in the absence and (B) in the presence of TN_{10}

3.3. Surface composition analysis

Figure 8A presents the surface morphology of Brass, after 24 h of immersion in 3% NaCl solution containing sulphide ions and in the absence of TN_{10} (reference solution). It can be seen that spongy corrosion products cover

the alloy surface. In contrast, in the presence of TN_{10} (Figure 8B), almost no corrosion is revealed, and the grooves due to the initial surface abrasion remain clearly visible after 24 h immersion. Some precipitates observed are NaCl crystals, because of insufficient surface rinsing. The comparison of these two figures reveals a marked inhibiting efficiency of TN_{10}.

CONCLUSION

An investigations on the effect of adding N-decyl-3-amino-1,2,4-triazole (TN10) to 3%NaCl solution containing sulphide ions reveal that it is an excellent inhibitor for Brass.

The presence of 2 ppm of sulphide ions accelerates the dissolution of the brass in 3%NaCl solution and leads to the formation of sulphur rich, non-protective film at the surface.

The inhibitor acts on the anodic and cathodic electrochemical processes. Polarisation curves showed that the inhibiting effect of this compound results in a clear reduction of the cathodic and anodic current density values especially near corrosion potential. A remarkable inhibiting effect of TN_{10} is observed when its concentration is higher than 0.1 mM. These results were confirmed by impedance tests where it was observed that the effect of inhibitor addition is distinguished by an increase of the resistance and a strong reduction of the electrochemical interface capacity value. Inhibition efficiency of this compound depends on its concentration. Indeed, it adsorbs on the Brass surface according to the Frumkin isotherm model.

The protective effect improves with immersion time, and reached values as high as 99% after 24 h of immersion time. Addition of TN_{10} inhibitor modifies the characteristics of the interface Brass in 3%NaCl in presence of sulphide ions. All these lead to propose formation of strong inhibiting film, which could protect the metal.

REFERENCES

[1] Li, S.L., Ma, H.Y., Lei, S.B., Yu, R., Chen, S.H., and Liu, D.X., *Corrosion*, **1998,** 54, 947-954.
[2] Milan M. Antonijević, Snežana M. Milić, Marija B. Petrović, *Corros. Sci*., **2009**, 51, 1228-1237.
[3] F. M. Kharafi, B. G. Ateya and R. M. Abd Allah, *J. Appl. Electrochem*., **2004,** 34, 47-53.
[4] M. Abdallah, M. Al- Agez and A.S. Fouda, *Int. J. Electrochem. Sci.*, **2009**, 4, 336-352.
[5] E. M. Sheriff and Su-Moon Park, *Electrochim. Acta*, **2006**, 51, 6556-6562.
[6] S. Mamas, T. Kiyak, M. Kabasakalogu and A. Koc, *Mater. Chem. Phys.*, **2005,** 93, 41-47.
[7] Vera R., Bastidas F., Villarroel M., Oliva A., Molinari A., Ramirez D., Rio A. R., *Corros. Sci.* **2008,** 50, 729-736.
[8] Alfantazi A. M., Ahmed T. M., Tromans D., *Mater. Des*. **2009**, 30, 2425-2450.
[9] Ali Davoodi, Saleheh Honarbakhsh, Gholam Ali Farzi. *Progress in Organic Coatings*, **2015**, 88, 106-115.
[10] Hongqiang Fan, Shuying Li, Zongchang Zhao, Hua Wang, Zhicong Shi, Lin Zhang. *Corrosion Science*, **2011**, 53, Issue 12, 4273-4281.
[11] L. Yohai, W. H. Schreiner, M. Vázquez, M. B. Valcarce, *Journal of Solid State Electrochemistry*. **2015,** 19, Issue 5, 1559-1568.
[12] X. Joseph Raj, N. Rajendran. *Protection of Metals and Physical Chemistry of Surfaces*. **2013,** 49, Issue 6, 763-775.
[13] M. Damej, D. Chebabe, M. Benmessaoud, A. Dermaj, H. Erramli, N. Hajjaji, A. Srhiri. *Corrosion Engineering, Science and Technology*. **2015**, 50, Issue 2, 103-107.
[14] Milan B. Radovanović, Marija B. Petrović, Ana T. Simonović, Snežana M. Milić, Milan M. Antonijević. *Environmental Science and Pollution Research*. **2013,** 20, Issue 7, 4370-4381.
[15] M. Damej, H. Benassaoui, D. Chebabe , M. Benmessaoud , H. Erramli, A. Dermaj, N. Hajjaji and A. Srhiri, *J. Mater. Environ. Sci*. **2016,** 7 (3), 738-745.
[16] S. Tamilselvi, V. Raman and N. Rajendran, *J. Appl. Electrochem.*, **2003,** 33, 1175-1182.
[17] M. M. Antonijevic, G. D. Bogdanovic, M. B. Radovanovic, M. B. Petrovic and A.T. Stamenkovic, *Int. J. Electrochem. Sci.*, **2009,** 4, 654-661.
[18] F. Bentiss, M.Lebrini, H. Vezin, M.Lagrenee, *Mater. Chem. Phys*., **2004,** 87, 18-23.
[19] M. G. Fontana, "Corrosion Engineering," 3rd Edition, McGraw-Hill Book Company, New York, **1987**.
[20] M. Dupart, F. Dabosi, F. Moran and S. Rocher, *Corrosion Nace*, **1981**, 37, 262-266.
A. Bonnel, F. Dabosi, C. Deslouis, M. Duprat, M. Keddam and B. Tribollet, *Journal of the Electrochemical Society*, **1983,** 130, No. 4, 753-761.
[21] M. Keddam, A. Srhiri, H. Takenouti, B.Trachli, in: 15th International Corrosion Congress, Granada, September **2002**, CD-Rom Proceedings, no. 700.
[22] K. Es-Salah, M. Keddam, K. Rahmouni, A. Srhiri, H. Takenouti, *Electrochim. Acta*, **2004,** 49, 2771-2778.

[23] M. Stern, A.L. Geary, *J. Electrochem. Soc*. **1957,** 104, 56-63.
[24] G. Kear, B.D. Barker, F.C. Walsh, *Corros. Sci*. **2004,** 46, 109-135.
[25] B. Trachli, M. Keddam, A. Srhiri, H. Takenouti, *Corros. Sci*. **2002,** 44, 997-1008.
[26] E. D_Elia, O.E. Barcia, O.R. Mattos, N. Pèbère, B. Tribollet, *J. Electrochem. Soc*. **1996**, 143, 961-967.
[27] G. Cordeiro, O.R. Mattos, O.E. Barcia, L. Beaunier, C. Deslouis, B. Tribollet, *J. Appl. Electrochem*. **1996,** 26, 1083-1092.
[28] H. Takenouti, *Electrochemistry (Japan)*, **1999**, 67, 1063-1072.
[29] M. Elbakri, R. Touir, M. Ebn Tohami, A. Srhiri and M. Benmessaoud, *Corrosion science*, **2008,** 50, 1538-1545.
[30] Z. Mountassir and A. Srhiri, *Corrosion science*, **2007,** 49, 1350-1361.
[31] K. Rahmouni, M. Keddam, A. Srhiri, H. Takenouti, *Corros. Sci*.**2005,** 47, 3249-3266.
[32] Aouial, H. Takenouti and A. Srhiri, *Physical and Chemical News*, **2005,** 23, 108-118.
[33] B. C. Syrett. *Corrosion science*, **1981,** 21, 187-209.
[34] F. Mansfeld, G. Liu, H. Xiao, C. H. Tsai, and B. J. Little. *Corrosion science*, **1994,** 36, 2063-2095.
[35] D. J. Schffrin, and S. R. Desanchez. *Corrosion*, **1985,** 41, 31-38.